THE JOURNAL OF PHYSICAL CHEMISTRY Letters

Letter

pubs.acs.org/JPCL

Observation of Organic Molecules at the Aerosol Surface

Yajing Wu,[†] Wanyi Li,[‡] Bolei Xu,[†] Xia Li,[†] Han Wang,[‡] V. Faye McNeill,*[,‡] Yi Rao,*[,†] and Hai-Lung Dai[†]

[†]Department of Chemistry, Temple University, Philadelphia, Pennsylvania 19122, United States

[‡]Department of Chemical Engineering, Columbia University, New York, New York 10027, United States

Supporting Information

ABSTRACT: Organic molecules at the gas-particle interface of atmospheric aerosols influence the heterogeneous chemistry of the aerosol and impact climate properties. The ability to probe the molecules at the aerosol particle surface in situ therefore is important but has been proven challenging. We report the first successful observations of molecules at the surface of laboratory-generated aerosols suspended in air using the surface-sensitive technique second harmonic light scattering (SHS). As a demonstration, we detect trans-4-[4-(dibutylamino)styryl]-1-methylpyridinium iodide and determine its population and adsorption free energy at the surface of submicron aerosol particles. This work illustrates a new and versatile experimental approach for studying how aerosol composition may affect the atmospheric properties.

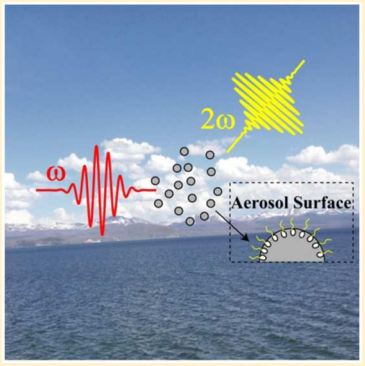

Particulate matter in Earth's atmosphere, also known as atmospheric aerosols, plays critical roles in air quality, climate, and atmospheric chemistry.[1−4] Organic materials comprise a significant fraction of small particle mass worldwide.[5−7] There is abundant indirect evidence that naturally occurring surface-active organic material resides preferentially at the gas-aerosol interface.[8] Atmospheric aerosols containing organic materials tend to consist of one or more liquid,[9,10] although solid or semisolid particles have also been observed.[11] Evidence also exists for liquid−liquid phase separation in mixed inorganic−organic aerosols, with an organic-rich outer layer surrounding an inorganic-rich inner core.[12] Organic materials at the gas−particle interface can influence atmospheric composition and climate by altering the heterogeneous chemistry, optical properties, and ice and cloud nucleating ability of atmospheric aerosols.[8,13] However, despite its importance, the chemical composition of the gas−particle interface has not been probed directly in situ due to a lack of suitable surface-sensitive analytical techniques.

Nonlinear optical methods such as second harmonic generation (SHG) and sum frequency generation (SFG) have been proven effective for investigating liquid or solid planar surfaces,[14−22] and more recently, in the form of second harmonic scattering (SHS) and sum frequency scattering (SFS) for surfaces of micro to nanometer size particles suspended in liquids.[23−27] These techniques have been applied to study liquid planar surfaces for mimicking atmospheric aerosols.[28−31] Recently, Geiger and co-workers used SFG to characterize the surface of atmospheric aerosols deposited on Teflon filters.[32] However, the use of these nonlinear optical techniques to probe the surface of aerosols suspended in gases has not been demonstrated yet. Observing aerosol interfacial composition in situ is desirable since collecting particles onto substrates for offline analysis can alter particle morphology and chemical properties due to relative humidity and temperature changes, loss of semivolatile material, or physical contact with other particles or the substrate itself.

The challenges in probing suspended aerosol particles using techniques such as SHS lie in the following: (1) the relatively low number density of particles gives low SHS signal, (2) the size of aerosols is typically around 100 nm, which is much smaller compared to the light wavelength and causes cancellation of the second harmonic light scattered off the particle surface, resulting in smaller collection efficiency; and 3) SHS from organic molecules without resonant enhancement is usually too low to be detected. Despite these challenges, we show in this report the first experimental detection of organic molecules at the surface of laboratory generated aerosols suspended in air.

A detailed description of our SHS experimental setup is found in the Supporting Information Sections S1 and S2. Briefly (see insert in Figure 1), a femtosecond (fs) 80 MHz Ti:sapphire oscillator (Coherent, Micra-5) was used to generate 50 fs fundamental light centered at 800 nm with an average power of 300 mW. The laser beam was tightly focused onto an aerosol flow with a focal length of 5 cm. The SHS signal was collected in the forward direction with a lens (2′ aperture, a focal length of 5 cm, 6 cm away from the aerosol flow). A blue glass filter and a spectrometer (PI, ACTON SP2300i) were used for wavelength selection for detection by a single-photon photomultiplier tube (PMT) and a single photon counter. Aerosols were generated by compressing liquid solutions through a constant output atomizer (TSI 3076) at a 4 L/min

Received: April 22, 2016
Accepted: June 1, 2016
Published: June 1, 2016

DOI: 10.1021/acs.jpclett.6b00872
J. Phys. Chem. Lett. 2016, 7, 2294−2297

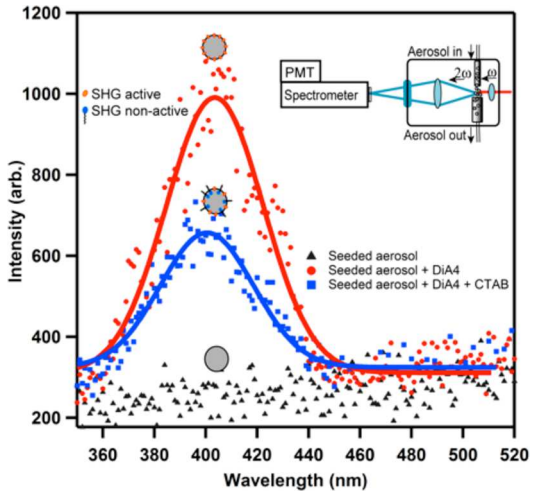

Figure 1. Emission spectra in the range of 350 to 520 nm collected from aerosols, under 800 nm light illumination, generated from three different solutions, including seeded aerosol, seeded aerosol with DiA4, and seeded aerosol with mixed DiA4 and CTAB. The emission spectrum of aerosols generated from 1 M NaCl solution (gray triangle) shows no peak at 400 nm. The emission spectrum of aerosols generated from the 20 μM DiA4 in 1 M NaCl solution (red circle) displays a peak centered at 400 nm. The spectral width is due to a broad fundamental 800 nm. After adding 20 μM CTAB into the DiA4 in NaCl solution, the SHS signals (blue square) decrease due to replacement of DiA4 by CTAB at the aerosol surface.

speed of pure N_2 gas. A PTFE tube introduces the aerosol flow into an enclosed chamber for SHS detection. A mechanical pump was used to evacuate the aerosol particles out of the chamber, and the flow rate of the pump was higher than the aerosols input rate to ensure that there were no residue aerosols left inside. A scanning mobility particle sizer (SMPS, TSI 3936) was used to measure size distribution of the aerosols. The average diameter of aerosols generated from 1 M NaCl solution was ~100 nm (see Supporting Information Section S3), and typical number densities were 10^7 particles per cm^3. As such, only 15−20 aerosol particles were collected in our experiments (see Supporting Information Section S4). The humidity in the chamber was maintained at 100% so that particles were not dried and remained aqueous after atomization until detection. *trans*-4-[4-(Dibutylamino)styryl]-1-methylpyridinium iodide (DiA4) was added into the 1 M NaCl solution to achieve desired concentrations.

DiA4, a SHG-active hemicyanine nonlinear chromophore,[33] is used as a probe molecule at the aerosol surface. The ground state absorption spectrum of DiA4 in water shows a strong absorption peak located at 475 nm corresponding to $S_0 - S_1$ absorption, and another band around 265 nm is also visible in the spectrum, which is attributed to $S_0 - S_n$ absorption (see Supporting Information Section S5). Since properties of aerosol surface are different from those at the air/water interface, a majority of the commonly used SHG probes at the air/water interface were found not to be an effective SHS probe at aerosol surface.

Figure 1 presents the emission spectra detected from the laboratory-generated aerosols illuminated with an 800 nm light. The peak at 400 nm, the wavelength where the SHS signal is expected, shows up from aerosols generated from 20 μM DiA4 in 1 M NaCl solution (red circle), whereas no peak is seen from aerosols without DiA4 molecules (gray triangle). We attribute this 400 nm peak to coherent SHS signals from the DiA4 molecules at the aerosol surface. To support the assignment of the SHS peak to the surface DiA4 molecules, we measured the SHS signal from aerosols generated from a DiA4 in NaCl solution in which another surface-active surfactant, cetyltrimethylammonium bromide (CTAB), is added. The addition of CTAB with a concentration of 20 μM is expected to replace DiA4 at the aerosol surface and subsequently causes a decrease in the SHS signal. This was indeed the observation. In addition, we have ruled out the possibility of reaction between DiA4 and CTAB that may lower the concentration of DiA4 molecules in bulk; signals at 400 nm detected from the bulk solutions of 20 μM DiA4 molecules dissolved in 1 M NaCl with and without CTAB were observed to be the same.

Upon irradiation of the 800 nm light, DiA4 would give a 400 nm SHS signal with resonance enhancement as well as two-photon excitation induced fluorescence (TPF). The DiA4 molecules at the aerosol surface should have similar orientations. Consequently, their second-order polarization will constructively interfere and give detectable SHS signal. For the DiA4 molecules in the bulk of the aerosol or a liquid solution, they are randomly orientated. Their second-order polarizations will sum up as zero in the coherent SHS process and subsequently no coherent SHS signal is expected. On the other hand, hyper-Rayleigh scattering (HRS), as an incoherent process, may still generate a detectable signal at 400 nm.[34,35] Both the HRS and the TPF signals are linearly proportional to the number of DiA4 molecules in the bulk solution.

We now examine the emission spectra in the range of 350 to 600 nm from aerosols and a bulk solution, which may consist of signals from SHS, HRS, or TPF. In Figure 2, the emission spectrum (gray triangles) detected from a bulk liquid solution of 20 μM DiA4 in 1 M NaCl solution in a quartz cuvette shows two peaks: A narrower band centered at 400 nm assignable to HRS from the DiA4 molecules in the bulk solution and a

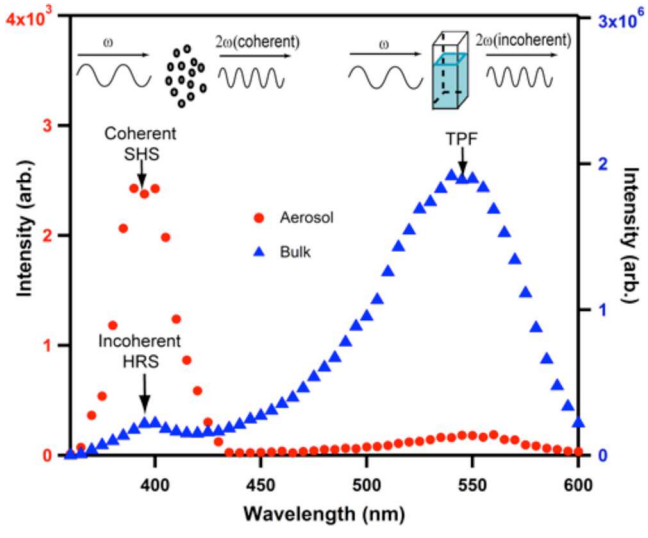

Figure 2. Emission spectra in the range of 350 to 600 nm detected from aerosols (red circle) and a bulk liquid solution (blue triangle), respectively, under 800 nm light illumination. The two-photon fluorescence signal at 550 nm is much stronger than the incoherent hyper-Rayleigh scattering signal at 400 nm for the bulk liquid solution. The 400 nm signal in the spectrum for the aerosols is attributed to the surface DiA4 molecules as the aerosol bulk DiA4 contributes negligible amount here based on the weak intensity of the TPF band.

DOI: 10.1021/acs.jpclett.6b00872
J. Phys. Chem. Lett. 2016, 7, 2294−2297

broader and much stronger band peaked at 550 nm assignable to DiA4 TPF. The intensities of the two bands are expected to keep the same ratio in different DiA4 concentrations. Figure 2 also displays the emission spectrum (red circles) from aerosol particles suspended in air, made from the same solution, under 800 nm illumination. There is relatively weak TPF band from aerosol particles because the amount of solution in aerosol particles is much less than that from the bulk solution. In contrast to the weak TPF, the signal at 400 nm is relatively strong. This peak should consist of contributions from both the SHS from the surface DiA4 and HRS from the bulk DiA4. The HRS contribution, based on the proportion to the TPF band intensity, to the 400 nm peak is negligible. The great majority of the 400 nm peak intensity should therefore arise from the SHS process of the DiA4 at the aerosol surface.

The population of DiA4 at the aerosol surface can be determined from a measurement of the SHS signal as a function of DiA4 concentrations in the aerosol. As a comparison, incoherent HRS signals were also measured for the bulk liquids solution at the same DiA4 concentrations.

Figure 3 compares integrated intensities of the 400 nm peaks detected from both the aerosols and the bulk liquid with the same DiA4 concentrations in the solution. The 400 nm intensity in the aerosol emission spectra, which arises primarily from the surface DiA4, as a function of the DiA4 concentration, was modeled according to the modified Langmuir adsorption isotherm[25] (Supporting Information Section S6). The isotherm model gives the number density of DiA4 molecules at surface (N_s), and the surface adsorption constant (K). A fit to the model yields the surface adsorption free energy of -9.68 ± 0.0002 kcal/mol and a density of $(2.5 \pm 0.2) \times 10^{14}$ molecules/cm^2 for DiA4 at the aerosol surface. On the other hand, the 400 nm intensity from the bulk solutions increase linearly with the DiA4 concentration, as expected from its assignment to the HRS process.

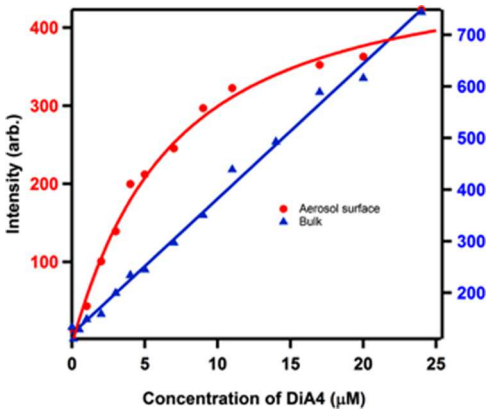

Figure 3. Intensities at the 400 nm peak as a function of DiA4 concentration from coherent SHS of aerosol surface (red circle) and incoherent HRS of bulk liquids (blue triangle), respectively. The red curve is a model fit of the SHS signal using the Langmuir adsorption isotherm, whereas the blue line represents a linear line as expected for the HRS signal.

On the basis of the effect of addition of the surfactant CTAB (Figure 1), the comparison of the aerosols and bulk liquid solution (Figure 2), and their concentration dependence (Figure 3), the 400 nm signal detected from the aerosols can be clearly assigned to DiA4 molecules at the aerosol surface and quantitatively analyzed for the determination of surface adsorption free energy and density. The demonstration of this experimental capability of using SHS to detect the presence of organic molecules at the surface of aerosols suspended in air is imperative for characterizing real environmental systems for understanding the growth of secondary organic aerosols. This experimental capability has the advantage, in addition to in situ surface sensitivity, of real-time resolution and will be versatile for directly studying structure, kinetics, dynamics, and photochemical reactions at the aerosol surface.

Even though we made significant progress to improve the collection efficiency of the SHS signal, still SHS-active molecules have to be used as a probe for the investigation of organic molecules at aerosol surface. SHS-active organic molecules can be probed directly, or alternatively, the SHS-inactive organic molecules can be probed as competition to the SHS-active molecules in surface adsorption.[36,37] Introducing SHS-active molecules into the aerosol system, as often done in life sciences,[38] could possibly bring complexity for the analysis at the aerosol surface. The next logical step is to develop SFG vibrational spectroscopy as a label-free, surface-sensitive probe to study environmentally meaningful molecules at the aerosol surface.

In summary, we have demonstrated that organic molecules at the surface of laboratory-generated aerosols suspended in air have been detected by using surface-sensitive second harmonic scattering. The adsorption free energy and density of the organic molecules at the aerosol surface have been quantitatively determined. This work illustrates a new approach for characterizing the aerosol surface in the atmosphere and represents a significant step toward establishing understandings of the interactions at the aerosol surface in atmospheric processes.

■ ASSOCIATED CONTENT

Supporting Information

The Supporting Information is available free of charge on the ACS Publications website at DOI: 10.1021/acs.jpclett.6b00872.

Descriptions of experimental setup, sample preparation and characterization, and calculations. (PDF)

■ AUTHOR INFORMATION

Corresponding Authors

*E-mail: yirao@temple.edu.

*E-mail: vfm2103@columbia.edu.

Notes

The authors declare no competing financial interest.

■ ACKNOWLEDGMENTS

This work is supported by the National Science Foundation grant CHE-1506789. The authors thank Dr. Dezheng Sun for helpful discussions. Y.R. thanks Dr. Greg Drozd for his help with the preparation of aerosols in the early stage of the program. W.L. (from Department of Environmental Science, Wuhan University, P. R. China) acknowledges a fellowship from the China Scholarship Council (CSC) for the participation in this research.

■ REFERENCES

(1) Seinfeld, J. H. *Atmospheric Chemistry and Physics: From Air Pollution to Climate Change*, 2nd ed.; Pandis, S. N., Ed.; Wiley: Hoboken, NJ, 2006.

DOI: 10.1021/acs.jpclett.6b00872
J. Phys. Chem. Lett. 2016, 7, 2294−2297

(2) Finlayson-Pitts, B. J. *Chemistry of the Upper and Lower Atmosphere Theory, Experiments and Applications*; Pitts, J. N., Ed.; Academic Press: San Diego, CA, 2000.
(3) Quinn, P. K.; Collins, D. B.; Grassian, V. H.; Prather, K. A.; Bates, T. S. Chemistry and Related Properties of Freshly Emitted Sea Spray Aerosol. *Chem. Rev.* **2015**, *115*, 4383−4399.
(4) Kahan, T. F.; Wren, S. N.; Donaldson, D. J. A Pinch of Salt Is All It Takes: Chemistry at the Frozen Water Surface. *Acc. Chem. Res.* **2014**, *47*, 1587−1594.
(5) McNeill, V. F. Aqueous Organic Chemistry in the Atmosphere: Sources and Chemical Processing of Organic Aerosols. *Environ. Sci. Technol.* **2015**, *49*, 1237−1244.
(6) Donaldson, D. J.; Vaida, V. The Influence of Organic Films at the Air-Aqueous Boundary on Atmospheric Processes. *Chem. Rev.* **2006**, *106*, 1445−1461.
(7) Jimenez, J. L.; et al. Evolution of Organic Aerosols in the Atmosphere. *Science* **2009**, *326*, 1525−1529.
(8) McNeill, V. F.; Sareen, N.; Schwier, A. N. Surface-Active Organics in Atmospheric Aerosols. *Top. Curr. Chem.* **2013**, *339*, 201−259.
(9) Marcolli, C.; Luo, B. P.; Peter, T. Mixing of the Organic Aerosol Fractions: Liquids as the Thermodynamically Stable Phases. *J. Phys. Chem. A* **2004**, *108*, 2216−2224.
(10) Zuend, A.; Marcolli, C.; Luo, B. P.; Peter, T. A Thermodynamic Model of Mixed Organic-Inorganic Aerosols to Predict Activity Coefficients. *Atmos. Chem. Phys.* **2008**, *8*, 4559−4593.
(11) Virtanen, A.; et al. An Amorphous Solid State of Biogenic Secondary Organic Aerosol Particles. *Nature* **2010**, *467*, 824−827.
(12) You, Y.; et al. Images Reveal That Atmospheric Particles Can Undergo Liquid-Liquid Phase Separations. *Proc. Natl. Acad. Sci. U. S. A.* **2012**, *109*, 13188−13193.
(13) George, C.; Ammann, M.; D'Anna, B.; Donaldson, D. J.; Nizkorodov, S. A. Heterogeneous Photochemistry in the Atmosphere. *Chem. Rev.* **2015**, *115*, 4218−4258.
(14) Shen, Y. R. Surface-Properties Probed by 2nd-Harmonic and Sum-Frequency Generation. *Nature* **1989**, *337*, 519−525.
(15) Chen, Z.; Shen, Y. R.; Somorjai, G. A. Studies of Polymer Surfaces by Sum Frequency Generation Vibrational Spectroscopy. *Annu. Rev. Phys. Chem.* **2002**, *53*, 437−465.
(16) Eisenthal, K. B. Liquid Interfaces Probed by Second-Harmonic and Sum-Frequency Spectroscopy. *Chem. Rev.* **1996**, *96*, 1343−1360.
(17) Richmond, G. L. Molecular Bonding and Interactions at Aqueous Surfaces as Probed by Vibrational Sum Frequency Spectroscopy. *Chem. Rev.* **2002**, *102*, 2693−2724.
(18) Heskett, D.; Song, K. J.; Burns, A.; Plummer, E. W.; Dai, H. L. Coverage Dependent Phase-Transition of Pyridine on Ag(110) Observed by 2nd Harmonic-Generation. *J. Chem. Phys.* **1986**, *85*, 7490−7492.
(19) Urbach, L. E.; Percival, K. L.; Hicks, J. M.; Plummer, E. W.; Dai, H. L. Resonant Surface 2nd-Harmonic Generation - Surface-States on Ag(110). *Phys. Rev. B: Condens. Matter Mater. Phys.* **1992**, *45*, 3769−3772.
(20) Wang, H. F.; Gan, W.; Lu, R.; Rao, Y.; Wu, B. H. Quantitative Spectral and Orientational Analysis in Surface Sum Frequency Generation Vibrational Spectroscopy (Sfg-Vs). *Int. Rev. Phys. Chem.* **2005**, *24*, 191−256.
(21) Gopalakrishnan, S.; Liu, D. F.; Allen, H. C.; Kuo, M.; Shultz, M. J. Vibrational Spectroscopic Studies of Aqueous Interfaces: Salts, Acids, Bases, and Nanodrops. *Chem. Rev.* **2006**, *106*, 1155−1175.
(22) Geiger, F. M. Second Harmonic Generation, Sum Frequency Generation, and Chi((3)): Dissecting Environmental Interfaces with a Nonlinear Optical Swiss Army Knife. *Annu. Rev. Phys. Chem.* **2009**, *60*, 61−83.
(23) Eisenthal, K. B. Second Harmonic Spectroscopy of Aqueous Nano- and Microparticle Interfaces. *Chem. Rev.* **2006**, *106*, 1462−1477.
(24) Gonella, G.; Dai, H. L. Second Harmonic Light Scattering from the Surface of Colloidal Objects: Theory and Applications. *Langmuir* **2014**, *30*, 2588−2599.
(25) Wang, H.; Yan, E. C. Y.; Borguet, E.; Eisenthal, K. B. Second Harmonic Generation from the Surface of Centrosymmetric Particles in Bulk Solution. *Chem. Phys. Lett.* **1996**, *259*, 15−20.
(26) Roke, S.; Gonella, G. Nonlinear Light Scattering and Spectroscopy of Particles and Droplets in Liquids. *Annu. Rev. Phys. Chem.* **2012**, *63*, 353−378.
(27) Rao, Y.; Kwok, S. J. J.; Lombardi, J.; Turro, N. J.; Eisenthal, K. B. Label-Free Probe of Hiv-1 Tat Peptide Binding to Mimetic Membranes. *Proc. Natl. Acad. Sci. U. S. A.* **2014**, *111*, 12684−12688.
(28) Kido Soule, M. C.; Hore, D. K.; Jaramillo-Fellin, D. M.; Richmond, G. L. Differing Adsorption Behavior of Environmentally Important Cyanophenol Isomers at the Air-Water Interface. *J. Phys. Chem. B* **2006**, *110*, 16575−16583.
(29) Hua, W.; Chen, X. K.; Allen, H. C. Phase-Sensitive Sum Frequency Revealing Accommodation of Bicarbonate Ions, and Charge Separation of Sodium and Carbonate Ions within the Air/Water Interface. *J. Phys. Chem. A* **2011**, *115*, 6233−6238.
(30) Shrestha, M.; Zhang, Y.; Ebben, C. J.; Martin, S. T.; Geiger, F. M. Vibrational Sum Frequency Generation Spectroscopy of Secondary Organic Material Produced by Condensational Growth from Alpha-Pinene Ozonolysis. *J. Phys. Chem. A* **2013**, *117*, 8427−8436.
(31) Hua, W.; Verreault, D.; Allen, H. C. Surface Electric Fields of Aqueous Solutions of Nh4no3, Mg(No3)(2), Nano3, and Lino3: Implications for Atmospheric Aerosol Chemistry. *J. Phys. Chem. C* **2014**, *118*, 24941−24949.
(32) Ebben, C. J.; et al. Organic Constituents on the Surfaces of Aerosol Particles from Southern Finland, Amazonia, and California Studied by Vibrational Sum Frequency Generation. *J. Phys. Chem. A* **2012**, *116*, 8271−8290.
(33) Paul, H. J.; Corn, R. M. Second-Harmonic Generation Measurements of Electrostatic Biopolymer-Surfactant Coadsorption at the Water/1,2-Dichloroethane Interface. *J. Phys. Chem. B* **1997**, *101*, 4494−4497.
(34) Das, P. K. Chemical Applications of Hyper-Rayleigh Scattering in Solution. *J. Phys. Chem. B* **2006**, *110*, 7621−7630.
(35) Terhune, R. W.; Maker, P. D.; Savage, C. M. Measurements of Nonlinear Light Scattering. *Phys. Rev. Lett.* **1965**, *14*, 681−684.
(36) Wang, H. F.; Troxler, T.; Yeh, A. G.; Dai, H. L. In Situ, Nonlinear Optical Probe of Surfactant Adsorption on the Surface of Microparticles in Colloids. *Langmuir* **2000**, *16*, 2475−2481.
(37) Jen, S. H.; Dai, H. L. Probing Molecules Adsorbed at the Surface of Nanometer Colloidal Particles by Optical Second-Harmonic Generation. *J. Phys. Chem. B* **2006**, *110*, 23000−23003.
(38) Lakowicz, J. R. *Principles of Fluorescence Spectroscopy*, 2nd ed.; Kluwer Academic/Plenum: New York, 1999.

DOI: 10.1021/acs.jpclett.6b00872
J. Phys. Chem. Lett. 2016, 7, 2294−2297